

# EMPIR project 18NRM02 PRISM-eBT: WP3 progress report – December 2021

Thorsten Sander

Web meeting on 14 December 2021

# Activities 3.1.x for PTB and AU

(pptx-slides prepared by Rolf Behrens, Thorsten Schneider, Jaroslav Šolc and Peter Georgi)

A1.2.1 (Dec 20) — Compile list of suitable transfer instruments for  $D_{w,1cm}$  measurements, select at least 2 small volume ionisation chambers

→ **A3.1.1 (Dec 20)** — Characterisation & calibration of at least 3 detectors (1 scintillator fully characterised by AU), 2 ionisation chambers and 1 diamond detector

→ **A3.1.2 (Mar 21)** — Development of a standardised traceable calibration process for commercially available small volume ionisation chambers at distances > 3 cm; results to be included in DIN 6803-3; *Monte Carlo simulations and measurements in water in progress for determination of correction factors*

→ **A3.1.3 (Aug 21)** — Determination of system specific quality correction factors for at least 3 different detectors ( 1 scintillator fully characterised by AU)

→ **A3.1.4 (Feb 22)** — Developm. of a stand. traceable calibr. process for scintillation and diamond detectors; results to be included in DIN 6803-3; *see MC information above*

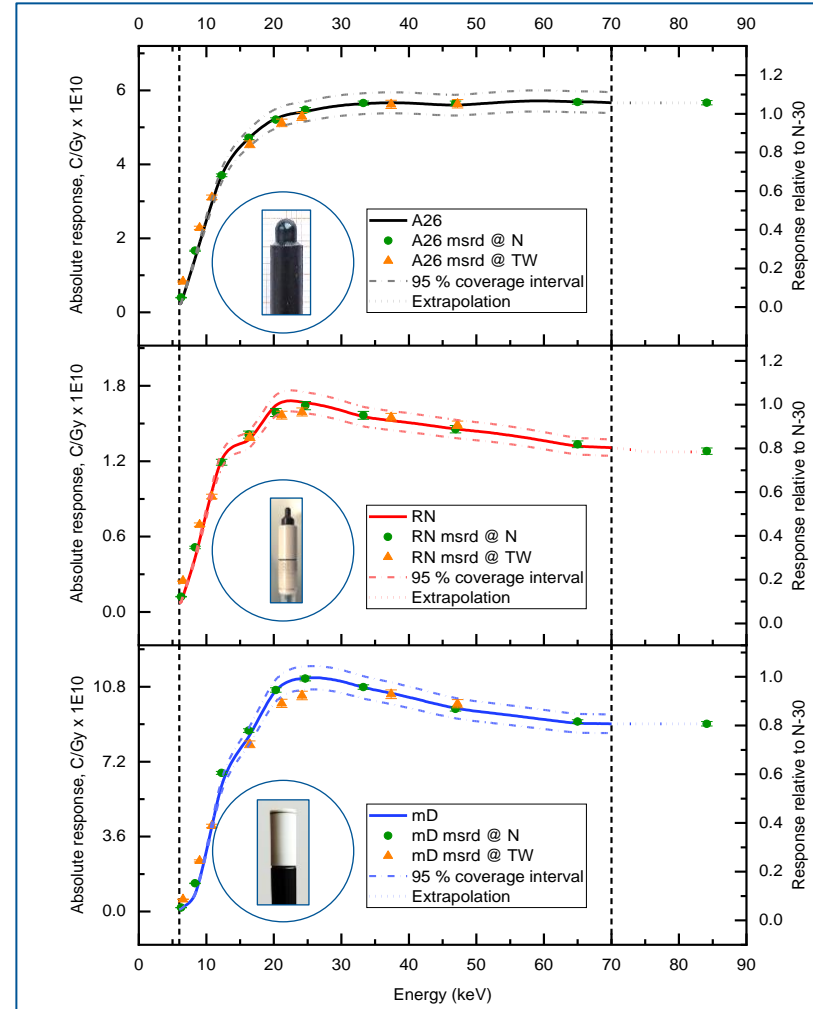
→ **A3.1.5 (Aug 22)** — Summary report on A3.1.1 to A3.1.4.

→ A3.3.6 (Dec 22) — Good Practice Guide (based on summary reports A3.x.5)

# WP3 progress (PTB)

## A3.1.1 (Dec 20) continued...

- The air kerma response of 3 small detectors was measured at low energy photon beams
- For the overall response all the calibration qualities (narrow and wide) are considered simultaneously using a Bayesian approach
- A paper on their suitability for eBT dosimetry has been submitted to PMB



Submitted for  
publication

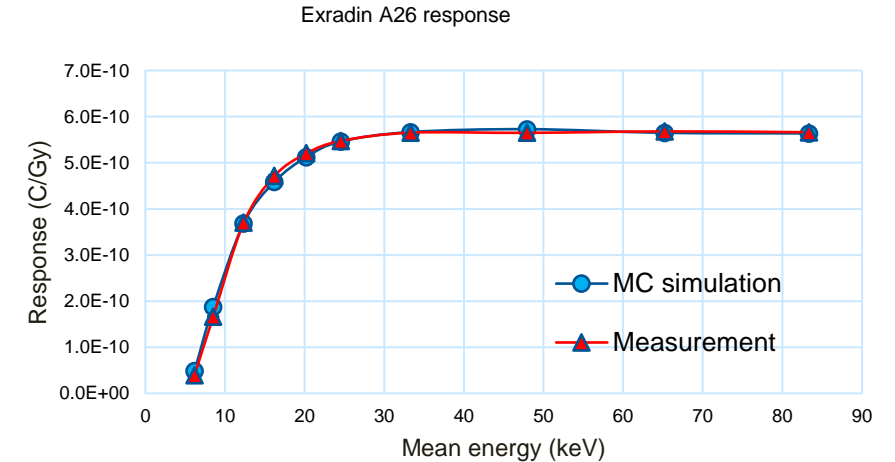
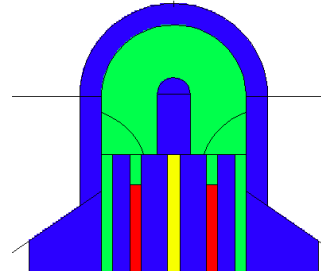
DRAFT

# WP3 progress (PTB, CMI)

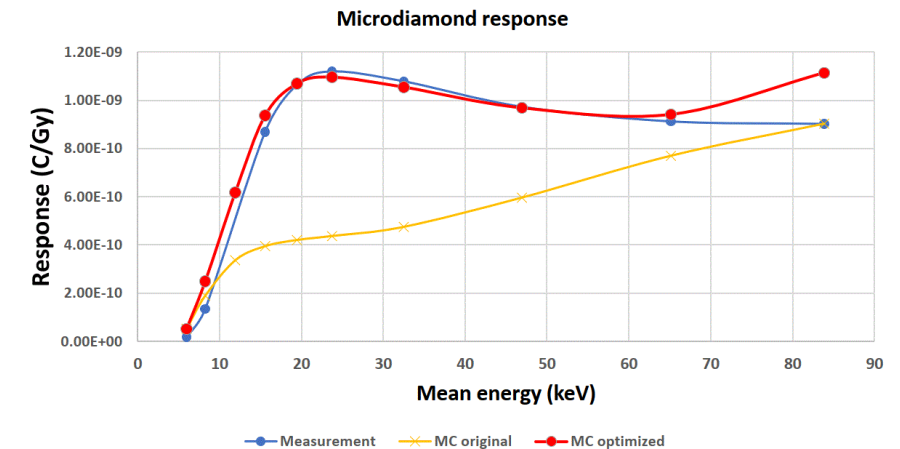
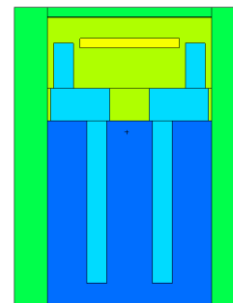
## A3.1.3 (Aug 21) - Determination of system specific quality correction factors

- Monte Carlo simulations (by Jaroslav Šolc, CMI) of the detectors in order to determine correction factors to convert the detector responses measured in terms of air kerma to absorbed dose to water
- The MCNP models of 2 detectors were validated with the response measured in air at PTB

A26



microDiamond



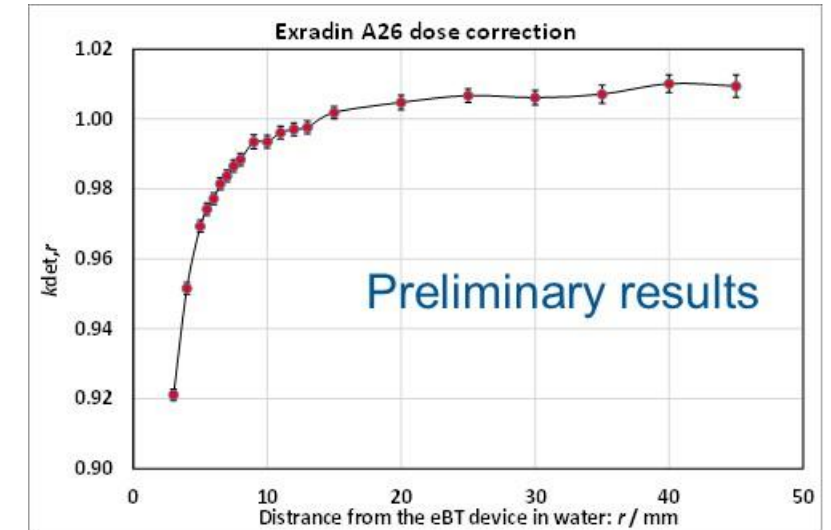
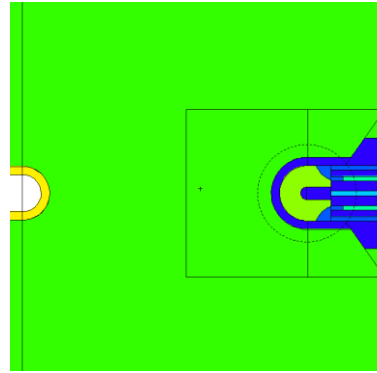
(Images from Jaroslav Šolc, CMI)

# WP3 progress (PTB, CMI)

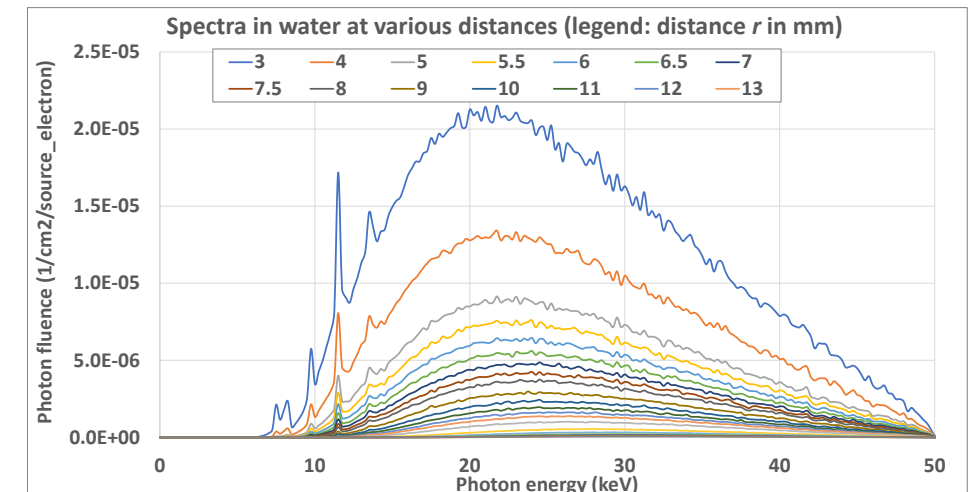
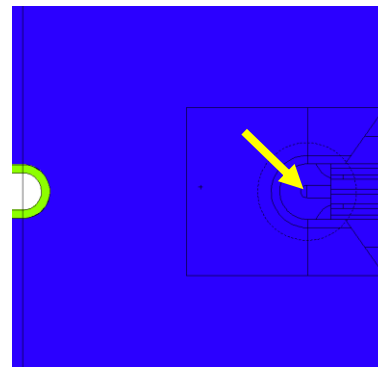
## A3.1.3 (Aug 21) - Determination of system specific quality correction factors

- Monte Carlo simulations (by Jaroslav Šolc, CMI) of the detectors in order to determine correction factors to convert the detector responses measured in terms of air kerma to absorbed dose to water
- Simulations in water using eBT spectra are ongoing to determine detector specific correction factors

A26 in air



A26 in/as water



(Images from Jaroslav Šolc, CMI)

# WP3 progress (AU)

## A3.1.1 (Dec 20)

P50 output as measured with PSD and WC

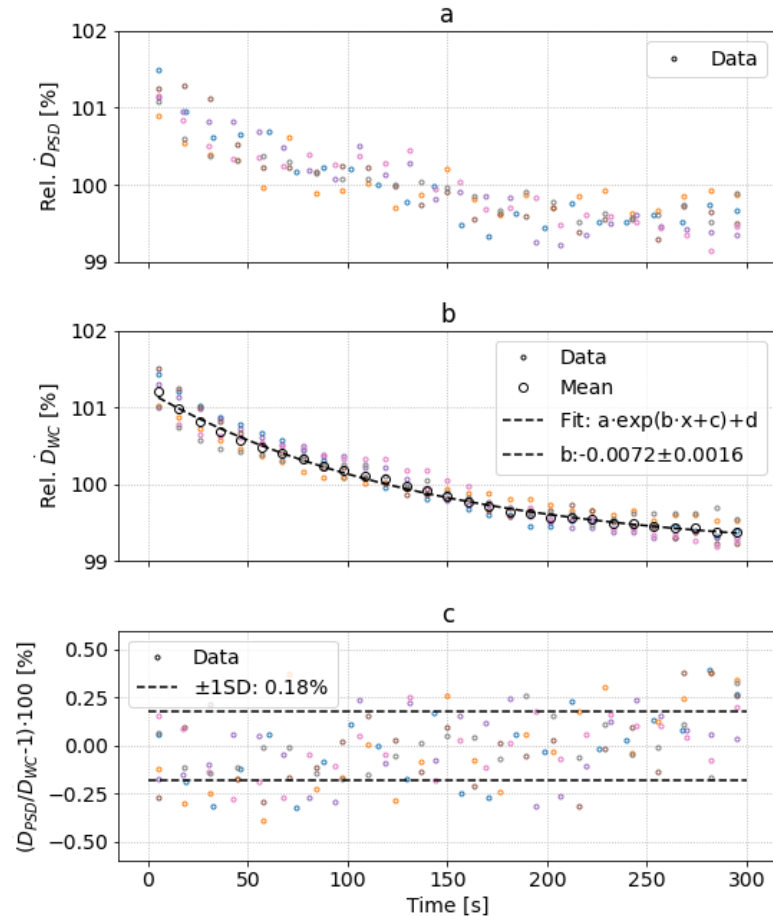


**Fig.1: P50 output temporal stability measured with PSD and WC**

### Detector characterisation:

1. Irradiate PSD and WC simultaneously for 300 s at P50 current 2.7 mA (clinical current). Gives temporal variation of P50 and stability of PSD, fig. 1.
2. Vary current between 0.3 mA and 3 mA and thereby vary dose-rate. Irradiate for 60 s. Compare PSD to WC to gain PSD stability and efficiency at varying dose-rates. Response drops linearly with increased dose-rate (fig. 3)!

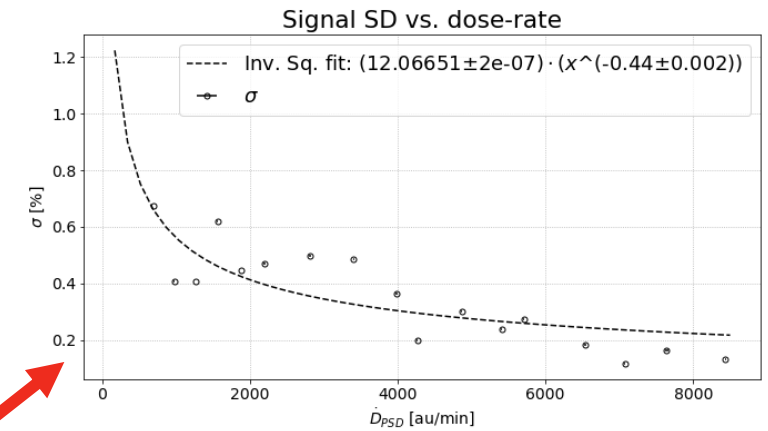
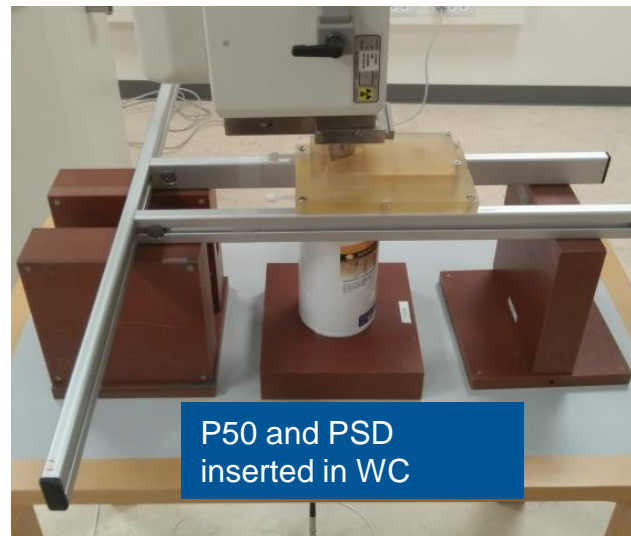


**Fig. 2: Uncertainty of PSD signal vs. measured dose-rate**

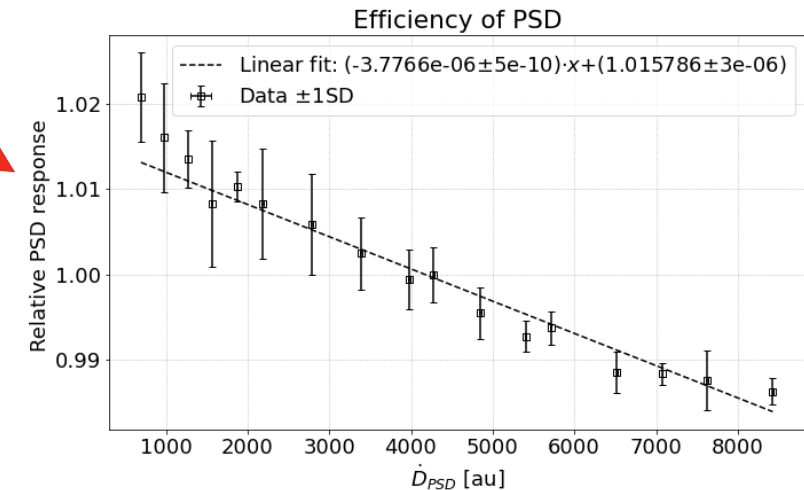


**Fig. 3: Relative efficiency of PSD vs. dose-rate,  $\dot{D}_{\text{PSD}}/\dot{D}_{\text{WC}}$**

# WP3 progress (AU)

## A3.1.1 (Dec 20)

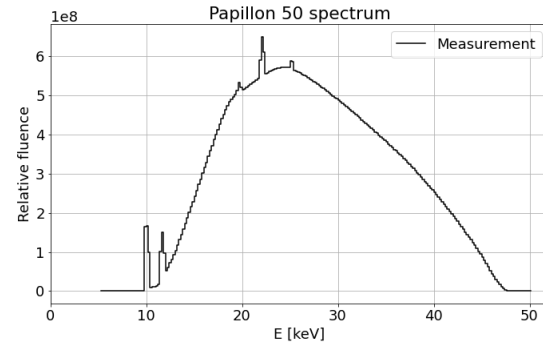


Fig. 4: P50 spectrum.

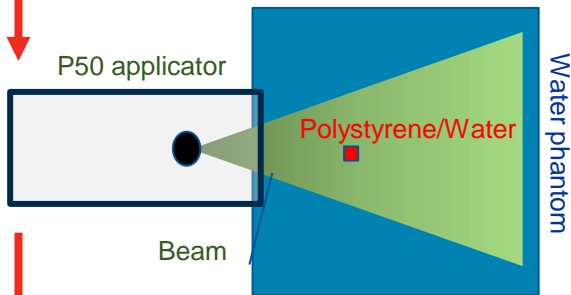


Fig. 5: Monte Carlo set-up sketch.

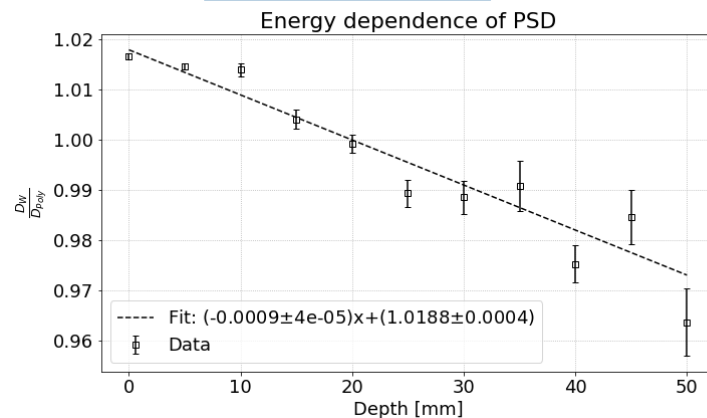


Fig. 6: Ratio of scored dose to water and polystyrene normalised at 20 mm depth.

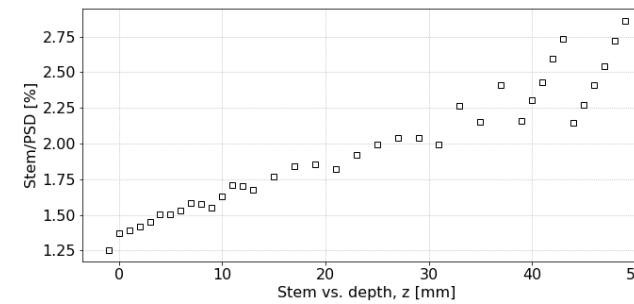
### System specific characterisation:

#### 1. Energy-dependence:

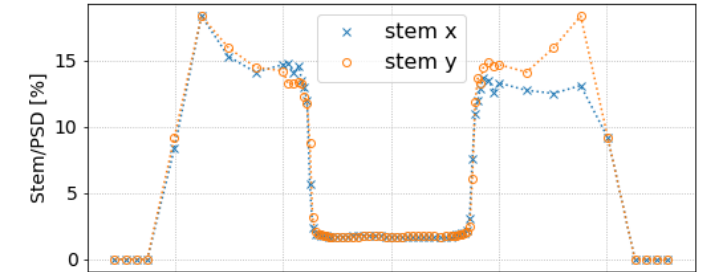
Obtained with TOPAS(Geant4) Monte Carlo simulation using P50 spectrum from PRISM-eBT catalogue measured by Jaroslav Šolc and Gustavo Kertzsch.

#### 2. Stem-effect:

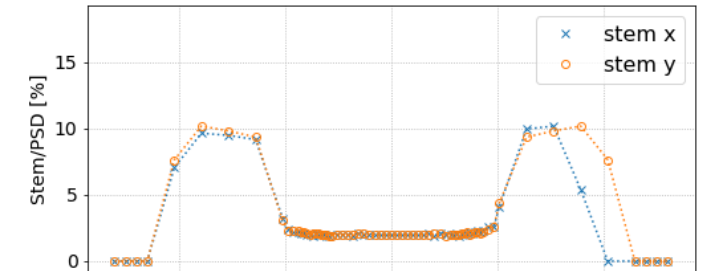
Obtained (and removed) with dummy probe without scintillating fibre. 1-3 % inside profile edges, 5-17% around edges and undetectable outside edges.



Profiles at z=5 mm



Profiles at z=20 mm



Profiles at z=50 mm

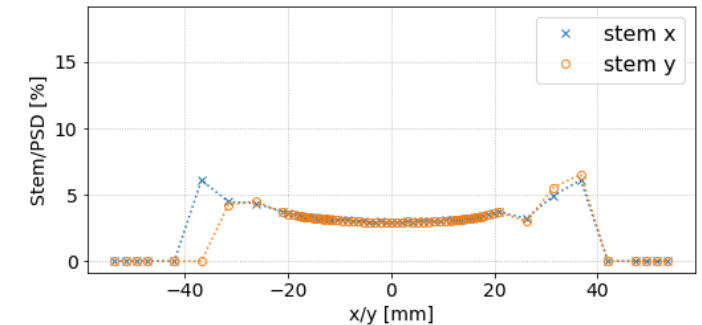


Fig. 7: Stem-effect contribution to measured signal along applicator central axis (top) and along profiles (rest).



# WP3 progress (AU)

## Continued...

- Uncertainty of reported dose (relative):  $D_{PSD} = ((S_{PSD} * L(\dot{S}_{PSD}) - S_{BG1}) - R_{PSD/BF} * (S_{BF} - S_{BG2})) * E$ .

Term	Description	Relative uncertainty contribution [%]
$S_{PSD}$	The raw signal from the PSD.	1.3
$L$	Dose-rate response correction factor.	1.7
$R_{PSD/BF}$	Normalisation factor for stem-effect in PSD and BF probe.	0.4
$S_{BF}$	The signal from the BF probe.	0.4
$S_{BG1}$	The background signal when measuring with PSD. Undetectable in current setup, and therefore set to the minimally detectable value.	0.5
$S_{BG2}$	The background signal when measuring with the BF probe. Undetectable in current setup, and therefore set to the minimally detectable value.	0.5
$E$	The energy-correction factor.	0.8
$D_{PSD}$	Conservative estimate of total uncertainty ( $\sqrt{\sum \sigma^2}$ )	2.5

## Submitted to Medical Physics

**3D Dose verification of an electronic brachytherapy source with a plastic scintillation detector**

### *Dosimetry for electronic brachytherapy*

Peter Georgi<sup>a)</sup>, Gustavo Kertzscher<sup>b)</sup>, Lars Nyvang<sup>b)</sup>, Jaroslav Šolc<sup>c)</sup>, Thorsten Schneider<sup>d)</sup>, Kari Tanderup<sup>a, b)</sup>, Jacob Graversen Johansen<sup>a, b)</sup>

a) Department of Clinical Medicine, Aarhus University, Aarhus, Denmark

b) Department of Oncology, Aarhus University Hospital, Aarhus, Denmark

c) Czech Metrology Institute, Brno, Czech Republic

d) WG 6.34 "Dosimetry for Brachytherapy and Beta Radiation Protection", Physikalisch-Technische Bundesanstalt (PTB), Braunschweig, Germany.



# Activities 3.2.x for CEA

(pptx-slides prepared by Valentin Blideanu)

A1.1.4 (Feb 22) — Development of  $D_{w,1cm}$  primary standards for eBT

**A3.2.1 (Jun 20)** — Determination of the effect of ageing of the Fricke gel on the dose sensitivity

**A3.2.2 (Dec 20)** — Monte Carlo calculations of absorbed dose and mean energy profiles in gel phantoms when irradiated in eBT-equivalent X-ray beams

**A3.2.3 (Dec 20)** — Experimental determination of correction factors for distortions in the MRI signal when reading out the Fricke gel dosimeter

**A3.2.4 (Dec 21)** — Calibration of the Fricke gel dosimeter in reference beam equivalent to INTRABEAM system with 40 mm diameter applicator ([scheduled for end 2021](#))

**A3.2.5 (Jan 22)** — Summary report on A3.2.1 to A3.2.4.

A3.3.6 (Dec 22) — Good Practice Guide (based on summary reports A3.x.5)

A4.1.6 (Dec 21) — Measurement of 3D  $D_{gel}$  dose distributions close to INTRABEAM system with 40 mm diameter applicator and conversion to absorbed dose to water

# WP3 progress (CEA)

## A3.2.2 (Dec 20)

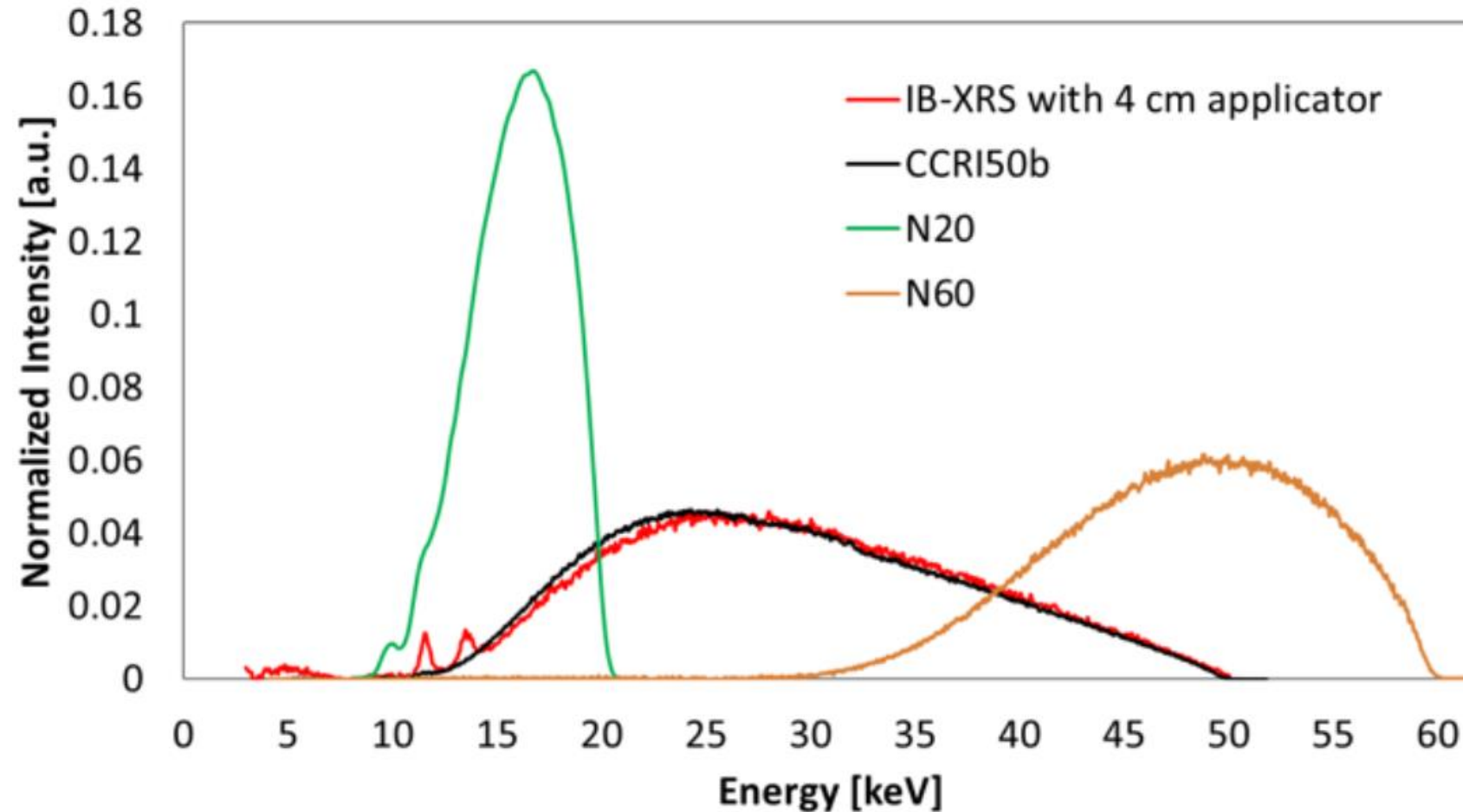


**Fig. 8: INTRABEAM equivalent beam (IB-XRS) compared to existing normalized beam qualities**

# WP3 progress (CEA)

## A3.2.2 (Dec 20) continued...

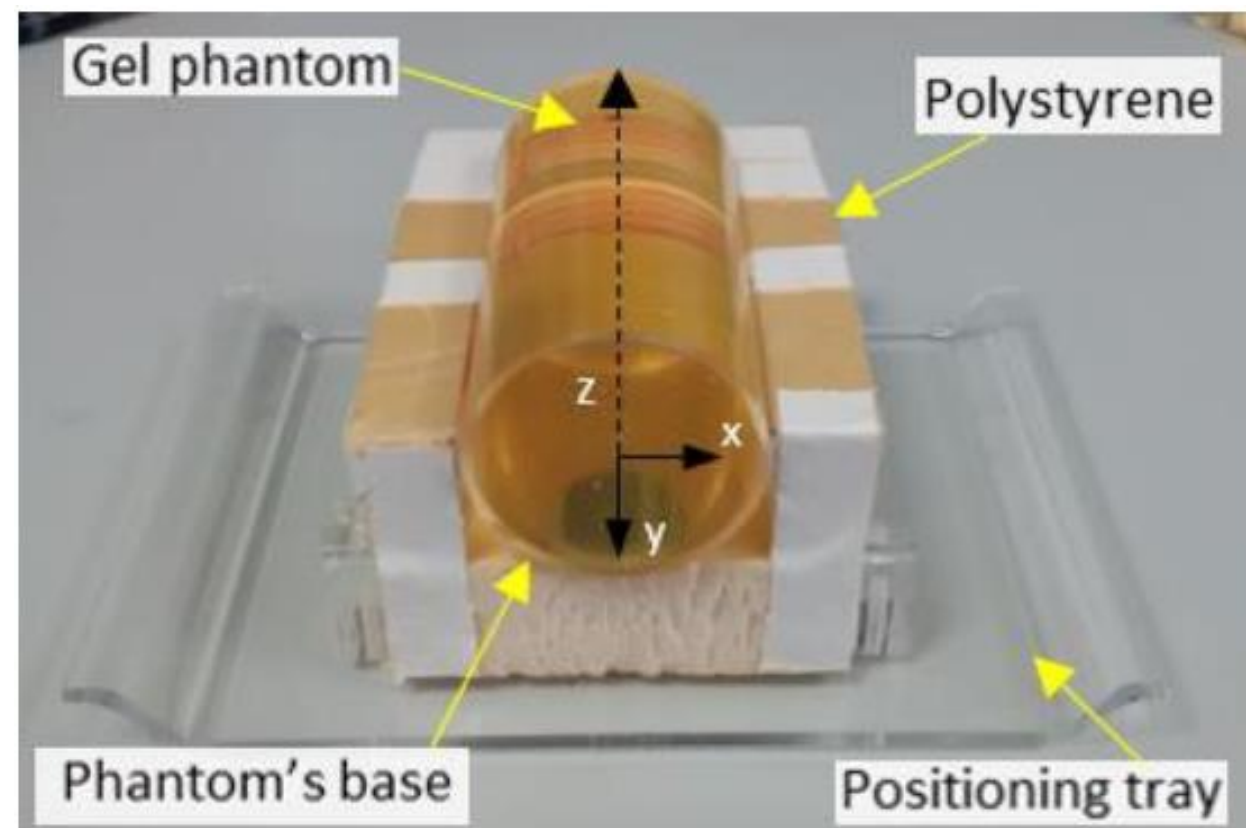
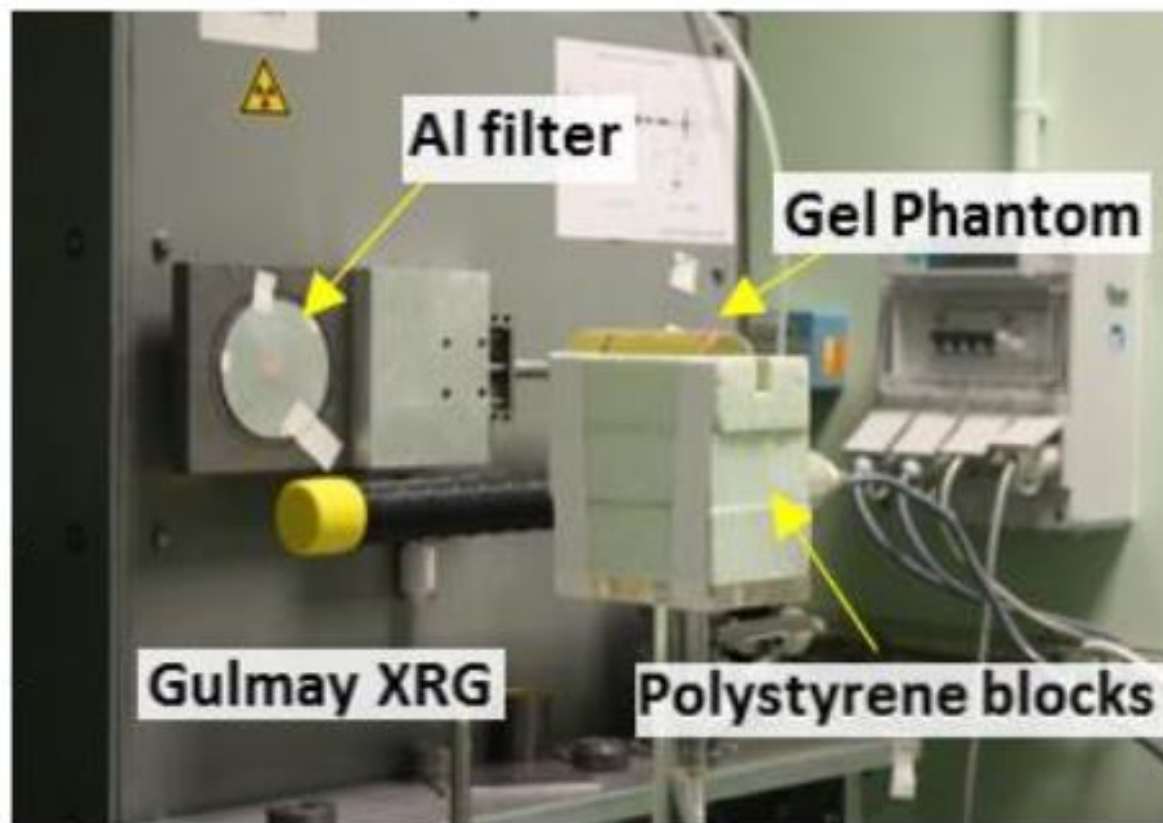


Fig. 9: Experimental set-up for gel irradiation

# WP3 progress (CEA)

## A3.2.2 (Dec 20) continued...

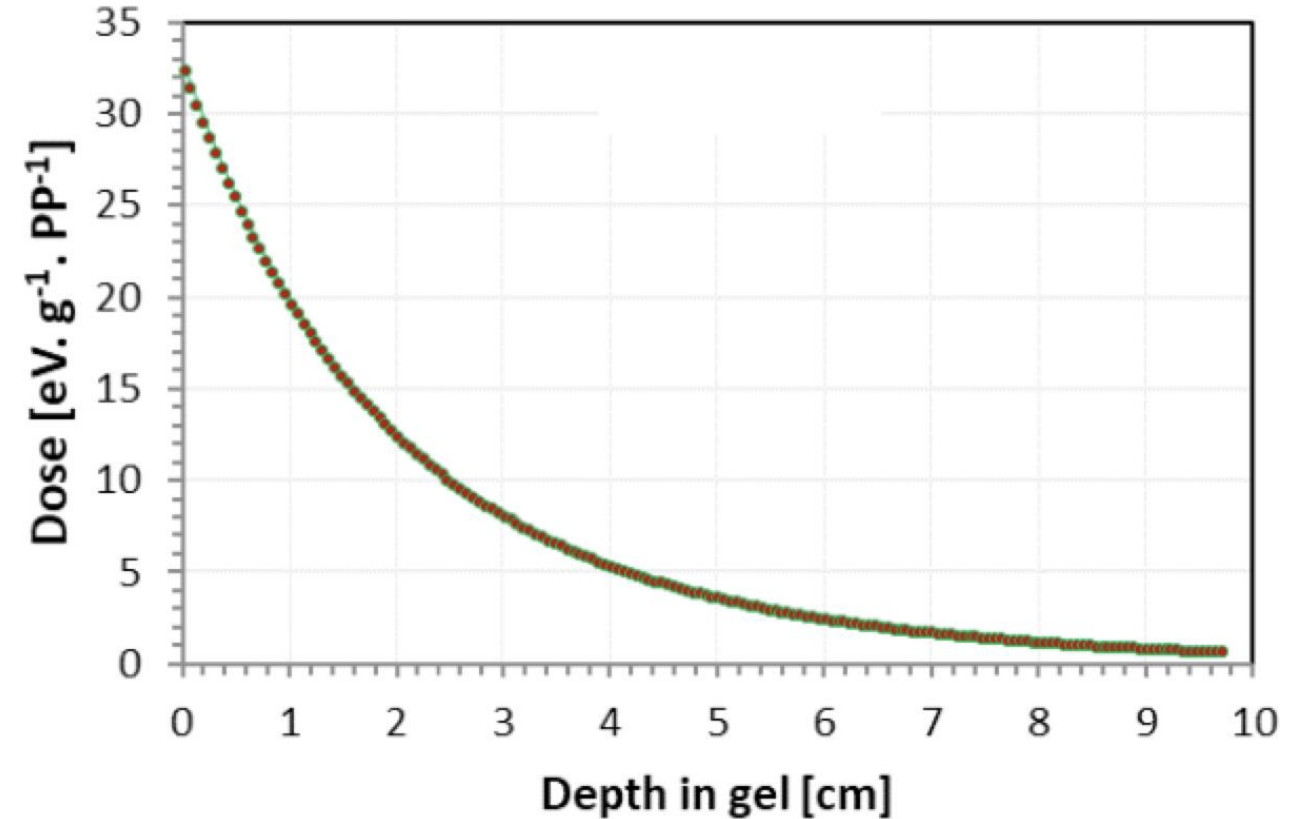
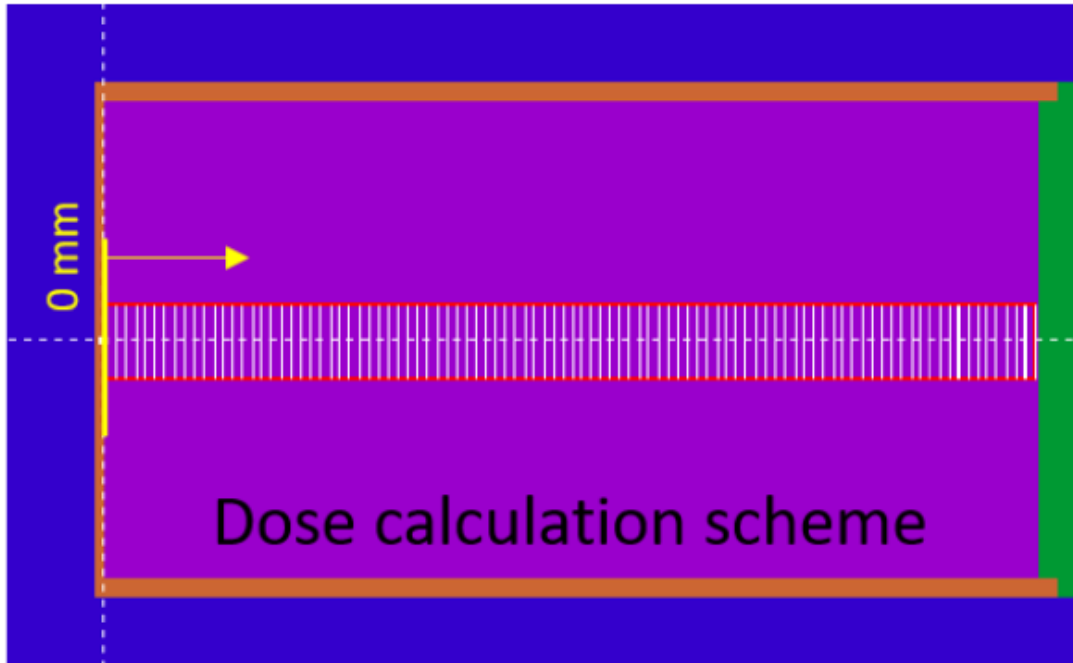


Fig. 10: Monte-Carlo model and calculation of absorbed dose distribution in gel phantom

# Activities 3.3.x for NPL

(pptx-slides prepared by Anna Subiel and Thorsten Sander)

A1.1.4 (Feb 22) — Development of  $D_{w,1cm}$  primary standards for eBT

A3.1.5 (Aug 22) — Summary report on A3.1.1 to A3.1.4.

A3.2.5 (Jan 22) — Summary report on A3.2.1 to A3.2.4.

**A3.3.1 (Nov 21) — Measurement of  $k_Q$  factors for eBT X-rays (using mono-E synchrotron radiation)**

→ **A3.3.2 (Nov 21) — Monte Carlo calculated  $k_Q$  factors for alanine for eBT X-rays**

→ **A3.3.3 (Dec 21) — Determine system specific quality correction factors for alanine (specific eBT source spectra from **CMI**, **MAASTRO clinic**, **PTB**)**

→ **A3.3.4 (Jul 22) — Write a paper on A3.3.1 to A3.3.3 and submit to peer-reviewed journal**

→ **A3.3.5 (Aug 22) — Summary report on A3.3.1 to A3.3.4.**

→ **A3.3.6 (Dec 22) — Good Practice Guide (based on summary reports A3.x.5)**

A4.1.2 (Jun 22) —  $D_w$  dose distribution measurements close to INTRABEAM (with & without applicator) and Papillon 50

A5.1.7 (Dec 22) — Submission of paper (A3.3.4)



# WP3 progress (NPL)

## A3.3.1 (Nov 21)

- Alanine characterisation at the DLS synchrotron using 8 - 20 keV monoenergetic X-rays in December 2019

- e-poster was presented at the International FLASH Radiotherapy & Particle Therapy conference, FRPT, Vienna, 1-3 December 2021



**Fig. 11: Diamond Light Source (synchrotron), Didcot, UK**

**ALANINE RESPONSE IN ULTRA-HIGH DOSE RATE (UHDR) LOW ENERGY SYNCHROTRON RADIATION**  
P. van den Eizen<sup>1,2,3</sup>, T. Sander<sup>1</sup>, H. Palmans<sup>1,2</sup>, M. McManus<sup>1</sup>, N. Woodall<sup>1</sup>, N. Lee<sup>1</sup>, O. Fox<sup>1</sup>, R. M. Jones<sup>1,2</sup>, D. Angel-Kalinin<sup>1,2</sup> and A. Sobel<sup>1</sup>  
<sup>1</sup> University of Manchester, Department of Physics and Astronomy, Manchester, United Kingdom; <sup>2</sup> The Cancer Research UK, University of Manchester, United Kingdom; <sup>3</sup> European Synchrotron Radiation Facility, Grenoble, France; <sup>4</sup> Australian Synchrotron, Victoria, Australia; <sup>5</sup> Diamond Light Source, Didcot, Oxfordshire, United Kingdom; <sup>6</sup> Science and Technology Facilities Council, Accelerator Science and Technology Centre, Sandhurst, United Kingdom

**Introduction**  
Low energy kV x-rays are regularly used in cases where their shallow dose penetration is desirable, such as intra-operative radiotherapy (IORT) and electronic brachytherapy (eBT). As the FLASH effect has been shown to occur in photon radiation<sup>1</sup>, pre-clinical studies using this radiation at very high dose-rates should take place using well-characterised dose-rate independent dosimeters. The alanine electron spin resonance (ESR) system fits the criteria as a reliable dose-rate independent dosimeter. The alanine response to low-energy kV x-rays relative to the calibration radiation (<sup>60</sup>Co) has been found to be strongly energy dependent. The response curve based on monoenergetic x-rays can be used to infer the relative response of alanine to more complex continuous x-ray spectra using convolution techniques.

**Method**  
Alanine pellets with 0.5 mm nominal and 5 mm diameter were irradiated on the beamline at the Diamond Light Source where 8 keV x-rays were used. A small portable graphitisation instrument was used as a reference transmission ionisation transfer instrument. The beam profile was determined by simulation of the setup and the

**Results**  
The response of alanine to monoenergetic 8 keV – 20 keV x-rays relative to the response to <sup>60</sup>Co radiation is shown in table 1. The data are given with a 95 % coverage factor. The largest contributions to the response are from the 8 keV and 10 keV components of the beam.

**Conclusion**  
The response of alanine to monoenergetic 8 – 20 keV x-rays relative to the response to <sup>60</sup>Co radiation has been determined. This will allow for alanine to be used as a dosimeter in pre-clinical work studying the FLASH effect with low-energy x-rays. This work is a foundation towards establishing alanine as a reliable dose-rate independent dosimeter for low-energy x-rays.

**Acknowledgements**  
This project 18NRM02 PRISM-eBT has received funding from the EMPIR programme co-financed by the Participating States and from the European Union's Horizon 2020 research and innovation programme. The project was also funded by the University of Manchester and the Science and Technology Facilities Council.

**Table 1: The relative response of alanine to monoenergetic x-rays with energies in the leftmost column. Uncertainties in the right columns are quoted with a coverage factor of 2.**

Energy (keV)	Relative response	Coverage factor
8	0.635	3.3
10	0.615	3.3
15	0.641	3.3
18	0.634	3.5
20	0.634	3.5

**Fig. 1: A picture of the setup used. Alanine pellets are embedded in a graphite block, mirroring the SPGC geometry. The beam travels from left to right.**

**e-poster presented at FRPT 2021, Vienna, 1 – 3 December 2021**  
**Unpublished results.**  
**Paper currently being written.**

[1] Montay-Gruel, P. et al., 2019, The FLASH effect: Ultra-high dose-rate ionising radiation prevents normal brain injury after whole brain irradiation in mice. *Nat. and Onc.*, 129(3), pp.582-585.

Contact details: p.vanden.eizen@npl.co.uk  
www.npl.co.uk

**NPL**  
National Physical Laboratory

**PRISM-eBT**

# WP3 progress (NPL)

## A3.3.1 and 3.3.2 (Nov 21) continued ...

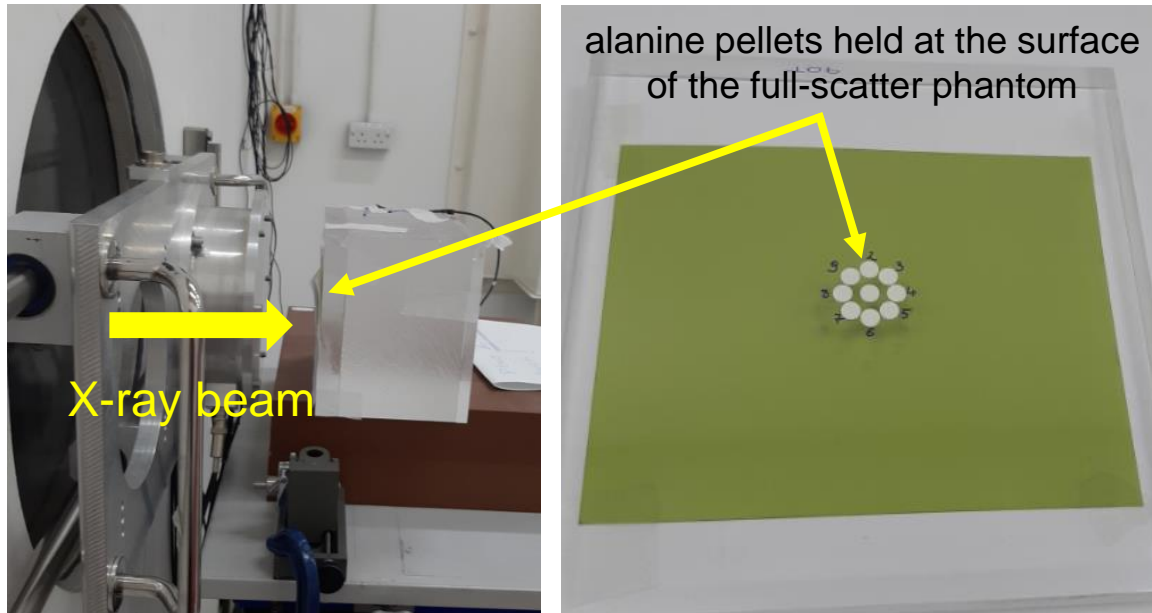


**Fig. 12: Experimental setup of alanine calibration at NPL**

- Due to lack of further access to DLS (due to Covid-19 pandemic) full energy characterisation (10 – 60 kV X-rays) has been carried out using NPL kV X-ray facilities employing ISO 4037 qualities (**N-10,N-15,N-20,N-25,N-40 and N-60 kV**) → for setup see **Fig. 12**
- Alanine pellets were cross-calibrated against a secondary standard 2611 ion chamber calibrated against primary standard FAC in terms of  $N_K$
- Conversion to  $D_w$  was carried out according to IPEM kV CoP
- Measurements completed
- Alanine pellets read out by NPL's Chemical Dosimetry Group using EPR system
- Now working on uncertainty budget



# WP3 progress (NPL)

## A3.3.1 and 3.3.2 (Nov 21) continued ...

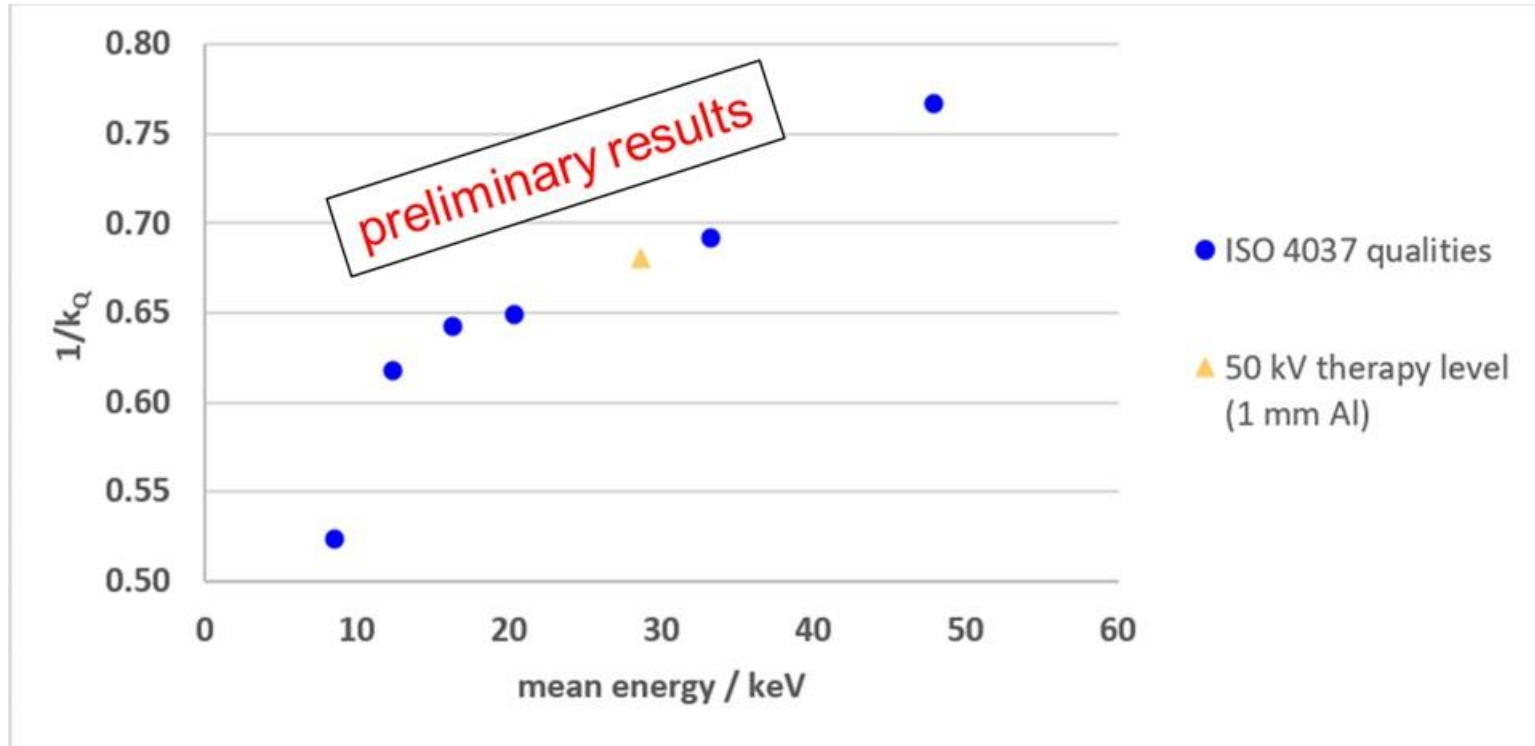


**Fig. 13: Alanine calibration at NPL based on ISO 4037 qualities: N-10,N-15,N-20,N-25,N-40 and N-60 kV**